Dyes and Pigments 92 (2012) 1314–1319

Contents lists available at SciVerse ScienceDirect

Dyes and Pigments

journal homepage: www.elsevier.com/locate/dyepig

Enhance the performances of dye-sensitized solar cell by a new type of sensitizer to co-sensitize zinc oxide photoelectrode with ruthenium complex

Lingyun Zhang[a,b], Yulin Yang[a,*], Ruiqing Fan[a,*], Ping Wang[a], Liang Li[a]

[a] Department of Chemistry, Harbin Institution of Technology, West Da-Zhi Street, Harbin 150001, PR China
[b] School of Chemical Engineering, Northeast Dianli University, Jilin 132012, PR China

ARTICLE INFO

Article history:
Received 7 August 2011
Received in revised form
4 September 2011
Accepted 9 September 2011
Available online 28 September 2011

Keywords:
Dye
Solar cell
Zinc oxide
Bis(imino) pyridine complexes
Co-sensitize
Photovoltaic

ABSTRACT

We designed a new type of sensitizer for dye-sensitized solar cells based on ZnO photoelectrode. Three five-coordinate transition metal complexes [2,6-(ArN=CMe)$_2$C$_5$H$_3$NMCl$_2$·nCH$_3$CN] (**M**=Zn, Cd, Hg) (named as **Zn1**, **Cd1**, **Hg1**), have been synthesized. In all complexes, the metal center is tridentately chelated by the ligand and further coordinated by two chlorine atoms, resulting in distorted trigonal bipyramidal geometry. The improvement in conversion efficiency of dye-sensitized solar cell was achieved by the complexes (**M**) and N719 co-sensitizing ZnO photoelectrode. In the tandem structure of **M**/N719/ZnO, the **M** forms a re-organization of energy level due to its single-crystal structure, which is advantageous to the electron injection and the hole recovery. The result demonstrates the **M**/N719 co-sensitized solar cell exhibited excellent photovoltaic performances with the short-circuit photocurrent density of 8.943 mA cm^{-2}, the open-circuit photovoltage of 591 mV and the fill factor of 0.639 under standard global AM 1.5 solar irradiation conditions.

1. Introduction

Over the past two decades, the dye-sensitized solar cell (DSSC) has attracted remarkable attention as one of the most promising technologies toward cost-effective solar energy exploitation [1,2]. The archetypal DSSC is composed of three key active components including mesoporous semiconductor film (for example, TiO_2, ZnO, SnO_2, Fe_2O_3), sensitizer and redox electrolyte. The mesoporous semiconductor film based on TiO_2 is the most extensively studied and is the most promising for photo-electron chemical systems [3,4]. Among the potential replacements for TiO_2, ZnO nearly has the same bandgap and electron affinity as TiO_2, but a higher chemical reactivity than TiO_2. Therefore, it is reasonable to expect mesoporous ZnO film could offer great potential toward the improvement of DSSC efficiency. Unfortunately, the efficiency of DSSC based on ZnO photoelectrode is much lower than that based on TiO_2 photoelectrode. In order to improve the efficiency of DSSC based on ZnO film, various methods have been used to carry out the ZnO photoelectrode, including the shape controlling [5–7], metal and metal oxide deposition [8–11], element doping [12–14], and light-scattering layer [15,16]. Shihe Yang et al. and other groups prepared nanowire, nanosheet, nanoflower, nanosphere, and nanorod ZnO with good linkage to improve the electron transfer speed. Au [8,9], MgO [11], and CuO [10] are coated on the surface of ZnO to form the core/shell composite, which provides an alternative pathway for electron to move across ZnO barrier. The elements (Ga [12], Al [13], and Sn [14]) doping for ZnO show substantial improvement in overall conversion efficiency compared with pure ZnO. More than 120% increase in the conversion efficiency has been achieved when single and double light-scattering lays are applied to ZnO-based DSSC [15]. The theoretical investigation and electron injection dynamics research discover the reason for the low efficiency of ZnO-based DSSC [17–19]. One of the most important reasons is the dye aggregation on the ZnO surface, which leads to slower electron efficiency from dye to ZnO [20,21]. One way to improve efficiency of DSSC is through the co-adsorption of dyes and structural modification with bulky substituent which can prevent p–p stacking or dye aggregation [22–24]. The co-sensitization approach is also very appealing for using multiple dyes to obtain panchromatic absorption. Porpyrin dye and various cyanine dyes are used to co-sensitize nanocrystalline TiO_2 films for improving photoelectric conversion efficiency [25–27]. Grätzel and coworkers co-sensitized nanocrystalline TiO_2 films with bisthiophene dye and squarylium cyanine dye and obtained the photoelectric conversion efficiency of 7.43%. This value is so far the highest value reported for co-sensitized DSSC with metal-coordination organic dyes [28].

* Corresponding authors. Tel./fax: +86 451 86413710.
E-mail addresses: ylyang@hit.edu.cn (Y. Yang), fanruiqing@hit.edu.cn (R. Fan).

0143-7208/$ – see front matter © 2011 Elsevier Ltd. All rights reserved.
doi:10.1016/j.dyepig.2011.09.007

In this paper, we present an approach to improve the efficiency through co-sensitizing ZnO photoelectrode with new type sensitizer to intensify the optical spectrum absorption. Three [bis(iminoalkyl)pyridine] ligand complexes [29,30] (**M**) reported before are used to sensitize the ZnO photoelectrode to form the carrier, then N719 dye sensitize the ZnO to form **M**/N719/ZnO tandem structure. The 2,6-bis(imino)pyridyl type of organic coordinate complexes co-sensitized ZnO with N719, form the composite photoelectrodes. The relationships between molecular structures and electrochemistry properties are further discussed. The **M**/N719/ZnO tandem structure shows a strong response in the UV region of the solar spectrum and much higher overall solar-to-energy conversion efficiency.

2. Experimental section

2.1. The synthesis of transition metal complexes

The 2,6-Diacetylpridine ligand was prepared according to a published procedure [31]. Free ligand, 2,6-(2,4,6-$Me_3C_6H_2N{=}CMe)_2C_5H_3N$, denoted as L was synthesized according to published procedures in a good yield by the condensation of 2, 6-diacetylpyridine with the corresponding aniline in refluxing absolute methanol in the presence of a catalytic amount of formic acid (Scheme 1) [29,30].

2.2. Preparation of ZnO powder

All the reagents were of analytical grade and used without further purification. ZnO was prepared according to the following solution-based procedure. 2.9747 g of $Zn(NO_3)_2{\cdot}6H_2O$ was dissolved in 200 ml of deionized water and then ammonia was added drop by drop with stirring until the pH was 7.0. The resulting white precipitate was isolated by centrifugation, washed with deionized water and ethanol, and dried at 320 °C for 2 h. Finally, the white powder of ZnO was obtained.

2.3. Photoelectrochemical measurements

The LiI, I_2, 4-tertbutylpyridine, acetonitrile, propylene carbonate, H_2PtCl_6 and fluorine-doped SnO_2 glass (FTO) are purchased from Aldrich Chemical Company. The *cis*-bis(isothiocyanato)bis[2,2-bipyridyl-4,4-dicarboxylate] ruthenium(II) bis-tetrabutylammonium known as N719 is received from Solaronix Company. A colloidal solution was obtained by mixing ZnO with ethanol (10wt%) and stirring for 12 h, then the colloidal solution was applied onto the conducting substrate (FTO) by the doctor blade technique. Adhesive tape was used as frame and spacer. The ZnO film was dry in air since there was no organic additive to burn up. The average cell of the film was 0.20 cm^2. The film electrodes were soaked in the transition metal complexes solution (concentration: 5×10^{-4} M, solvent mixture: acetonitrile and absolute ethanol in volume ratio of 1:1) for 3 h and N719 solution (concentration: 5×10^{-4} M, solvent mixture: acetonitrile and absolute ethanol in volume ratio of 1:1) for 3 h at room temperature, respectively. Then, the sensitized films were dry in air. The counter electrodes were a thermally platinized conducting glass (5 mM H_2PtCl_6 in dry isopropanol, heated at 400 °C for 10 min). The electrolyte was consisted of 0.5 M LiI, 0.05 M I_2, 0.1 M 4-tertbutylpyridine in 1:1 (volume ration) acetonitrile–propylene carbonate. The *J–V* curse of the sealed cells was measured under AM 1.5 illumination (100 mW cm^{-2}) using a solar simulator. Based on *J–V* curve, the fill factor (*FF*) is defined as: $FF = (J_{max} \times V_{max})/(J_{sc} \times V_{oc})$ where J_{max} and V_{max} are the photocurrent density and photovoltage for maximum power output (J_{sc} and V_{oc} are the short-circuit photocurrent density and open-circuit photovoltage, respectively.) $\eta = (FF \times J_{sc} \times V_{oc})/P_{in}$ the overall energy conversion efficiency (P_{in} is the power of incident light).

Electrochemical measurements were carried out on working electrode (chi660d, Chenhua, shanghai) with three-electrode system in the dark. Frequency range was 0.05–105 Hz, and the applied potential was generally between 0 and 0.700 V. The amplitude of AC signal was 10 mV. The Zview software was employed to fit the impedance.

Cyclic voltammetry measurement was carried out working electrode in CH_2Cl_2 (Aldrich, anhydrous, 99.8%) solution containing 0.1 M teterabutylammonium hexafluorophosphate (TBAPF6, Fluka, electrochemical grade) as an electrolyte. A mixed solvent system was employed to prevent adsorption to the electrode. The analyte concentration of typically 1 mM was used.

3. Results and discussion

3.1. Photoelectrochemical measurements

The transition metal complexes (**M**) were assembled onto the ZnO films to prepare the **M**/N719 co-sensitized photoelectrodes for dye-sensitized solar cell application. Fig. 1 presents the performances of the DSSC in terms of J_{sc} and V_{oc} in the transition metal complexes. The results in Table 1 indicate that the cell performances of DSSC co-sensitized with a mixture of transition metal

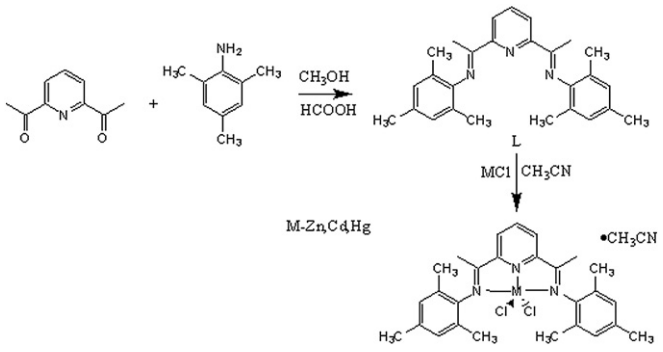

Scheme 1. Synthesis process of the transition metal complexes.

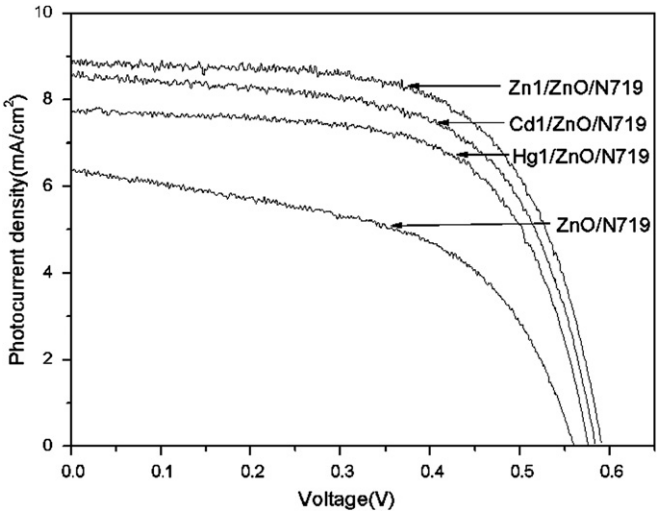

Fig. 1. *J–V* curves for dye-sensitized solar cell with different organometallic ligand complexes.

Table 1
J–V performances of **M**/N719/ZnO and raw ZnO photoelectrodes.

Photoelectrode	V_{oc}/mV	J_{sc}/mA cm^{-2}	*FF*	η/%
N719/ZnO	567	6.425	0.524	1.909
Zn1/N719/ZnO	591	8.943	0.639	3.378
Cd1/N719/ZnO	584	8.661	0.620	3.136
Hg1/N719/ZnO	577	7.811	0.644	2.907

complex and N719 are improved with fewer protons in center metal elements. The results of photochemical performances indicate that the co-sensitized solar cells based on the **M**/N719/ZnO electrode yield a remarkably high photocurrent density (J_{sc}) and open-circuit voltage (V_{oc}) under standard global AM 1.5 solar irradiation conditions. The **Zn1**/N719/ZnO composite photoelectrode is selected as an example to illustrate the effect of **M** on the performances of the DSSC. The J_{sc} and V_{oc} of co-sensitized solar cells based on the **Zn1**/N719/ZnO electrode are 8.943 mA cm^{-2} and 591 mV, respectively; the overall solar-to-energy conversion efficiency is 3.378%, which is much higher than that for the DSSC using single organic sensitizer (1.909%). With decrease of the proton number in the central metal atoms, the photochemical performances of composite photoelectrode are increasing. This result suggests that

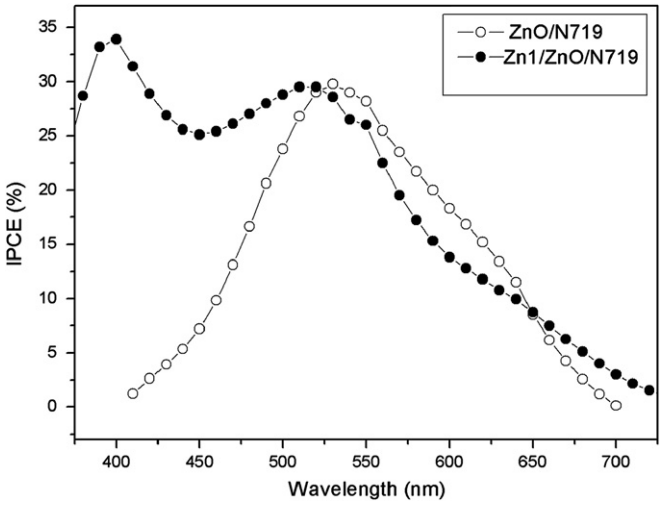

Fig. 2. IPCE spectrum of N719/ZnO and **Zn1**/N719/ZnO photoelectrodes based DSSC.

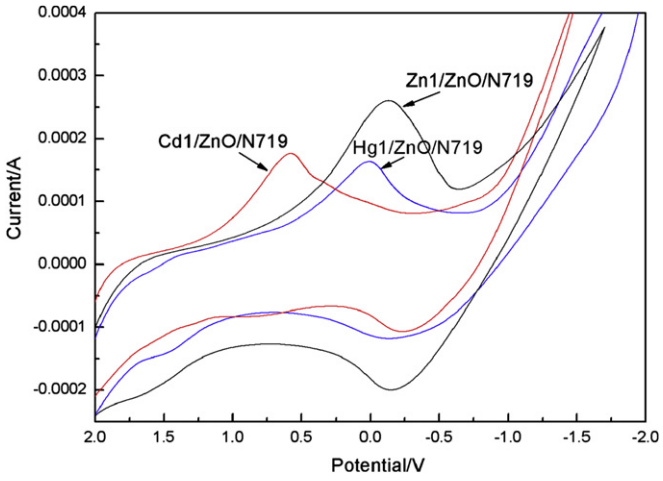

Fig. 3. Cyclic voltammograms of the metal complexes and blank sample in CH_2Cl_2 containing 0.1 M $TBAPF_6$ solution.

Table 2
Peak potentials of cyclic voltammograms for **Zn1**, **Cd1**, and **Hg1**.

Complex	E_{PC}/V	Epa/V	ΔEp/V
Zn1	−0.217	0.589	0.806
Cd1	−0.158	0.128	0.286
Hg1	−0.153	0.017	0.170

the complex/N719 co-sensitized ZnO photoelectrode is an effective way to improve the efficiency of DSSC.

To clarify the reason for a higher photocurrent of the solar cell based on the **M**/N719/ZnO electrode, we measured the incident photon-to-current conversion efficiency (IPCE). IPCE could be expressed in terms of the light-harvesting efficiency, the quantum yield of charge injection from the excited dye to the semiconductor, and the collection efficiency of injected electrons at the back contract. As can be seen from the spectra in Fig. 2, the spectrum shape of **Zn1**/N719/ZnO is obviously different from that of N719/ZnO. **Zn1** is absorbed on ZnO surface and displayed good result in **Zn1** and N719 co-sensitized solar cell. In Fig. 2, the IPCE spectrum for DSSC using **Zn1**/N719 exhibits two high peaks, 35% at 400 nm and 30% at 530 nm, respectively. IPCE spectrum for DSSC using **Zn1**/N719 exhibits an upward shift in the wavelength range from 300 nm to 500 nm. It shows that **Zn1**/N719 dye have higher light-harvesting efficiency and the quantum yield of charge injection. The result also demonstrates that co-sensitization for ZnO could construct with a higher UV–visible light activity over DSSC containing an individual dye. The use of dyes with efficient light-harvesting properties at low energies and negligible intermolecular interactions is important for the development of efficient multidye solar cell.

3.2. Cyclic voltammetric measurements

In order to explore the electrochemical behavior of the complexes, we carried out a cyclic voltammetric measurement. As

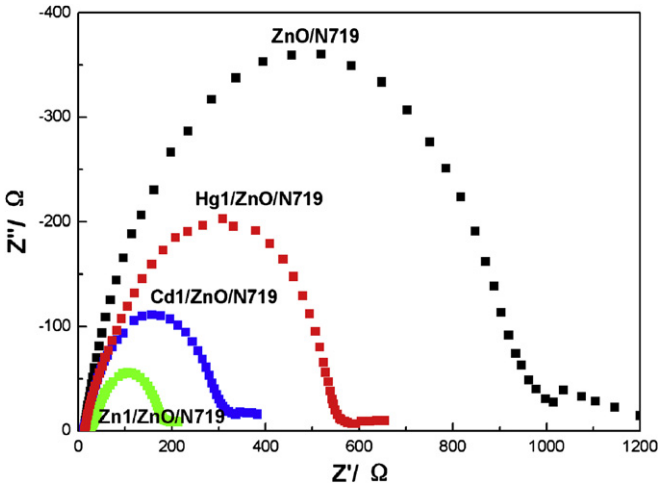

Fig. 4. Nyquist plots of the metal complex/N719 co-sensitized DSSC in standard global in the dark.

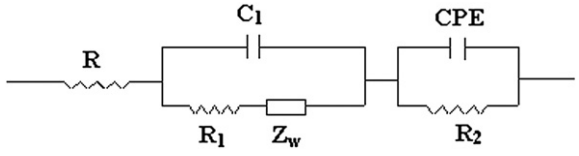

Fig. 5. Equivalent circuit used to model this system, representing interfaces in composite solar cell composed of FTO|ZnO/**M1**-dye|I_3^-/I^-||Pt|FTO.

Table 3
Parameters obtained by fitting the impedance spectra of composite solar cells using the equivalent circuit.

DSSC samples	R_s/Ω	C_1/F	R_1/Ω	$Y_{o,1}/S$	B/S	R_2/Ω	$Y_{o,2}/S$	n
N719/ZnO	14.20	6.70E-5	263.90	0.00079	0.25	421.40	5.63 E-4	0.66
Zn1/N719/ZnO	9.42	4.59E-4	93.02	0.09072	1.57	69.10	3.38 E-3	0.44
Cd1/N719/ZnO	11.35	1.51E-4	184.20	0.00515	3.97	95.01	6.85 E-4	0.65
Hg1/N719/ZnO	12.18	9.78E-5	250.40	0.01129	9.18	283.80	1.16 E-4	0.73

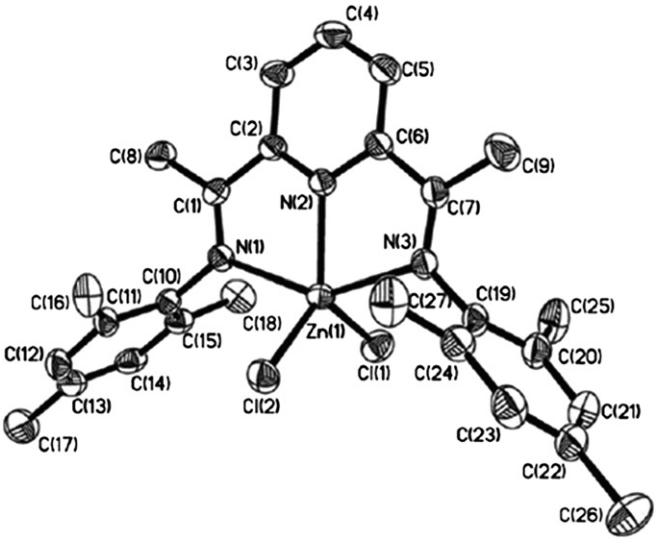

Fig. 6. Asymmetric unit of **Zn1**[30].

shown in Fig. 3, the cyclic voltammetric measurement was carried out by using a Pt electrode in aceonitrile solution containing 0.1 M tetrabutylammonium tetrafluorobarate as an electrolyte with the scan rate of 100 mV/s at room temperature. Table 2 lists cyclic voltammetric data of the transition metal complexes. The spectra show that all isopolyanions underwent one-step three-electron transition metal reduction process. **Zn1** presents similar electrochemical behavior to that of **Cd1** and **Hg1** in the aqueous solution, implied that the polymeric structures of the compounds are nearly identical. The LUMO level of the **M** species is from its redox potential by using cyclic voltammetry. The redox potential of **Zn1**, **Cd1**, and **Hg1** is −0.217 eV, −0.158 eV, and −0.153 eV, respectively. The negative redox potential of the complex is favorable for the high overall solar-to-energy conversion efficiency. High quantum efficiency for injection is achieved when the LUMO of the dye is both energetically matched and reasonably strongly coupled to the underlying semiconductor. The high LUMO level of the complex provides a favorable energy matching with the conduction level of ZnO for the electron transfer from the LUMO to the conduction band of ZnO.

Electrochemical impedance spectroscopy (EIS) has been widely used to correlate device structure with a suitable model for the study of the kinetics of electrochemical and photoelectrochemical processes occurring in DSSC. Impedance data were plotted on a Nyquist diagram. The fit and simulation processes are achieved using ZSimpWin software. In Fig. 4, experimental data are represented by symbols while the equivalent circuit is $R_s(C_1(R_1O_1))(R_2Q_2)$ (in Fig. 5). The spectrum shows one large semicircle at low frequency region and a small one at high frequency region. The diameter of semicircle decreases with the decreasing of protons of center metal atoms. The arcs tend to shrink with increasing J_{sc} because of the increasing number of electrons injected to ZnO. The equivalent circuit is a useful tool for understanding the output performance of solar cell and for further comprehension of the electrical behavior of DSSC. In equivalent circuit, the symbols R and C describe resistance and capacitance, respectively; O, which depends on the parameters $Y_{o,1}$ and B, accounts for a finite-length Warburg diffusion (Z_{Dif}), and Q is the symbol for the constant phase element, CPE (its parameters are $Y_{o,2}$ and n). R_s describes the series resistance for the dye-sensitized solar cells, and the elements with subscripts 1 and 2 are related, respectively, to the contribution of the interfaces of counter-electrolyte and porous electrode/electrolyte. Table 3 lists parameters obtained by fitting the impedance spectra of composite solar cells using the equivalent circuit in Fig. 5. This suggests that the high performances in DSSC sensitized with **M**/N719 are not only due to enhancement of spectral response in the UV region but also due to decrease of internal cell resistance.

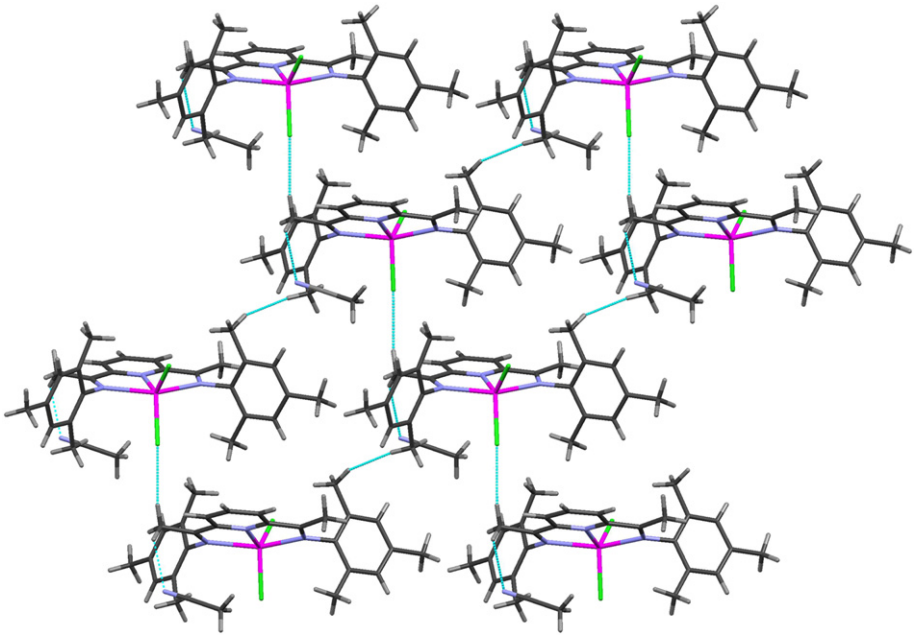

Fig. 7. Packing diagram of the complex **Zn1** along the *c* axis.

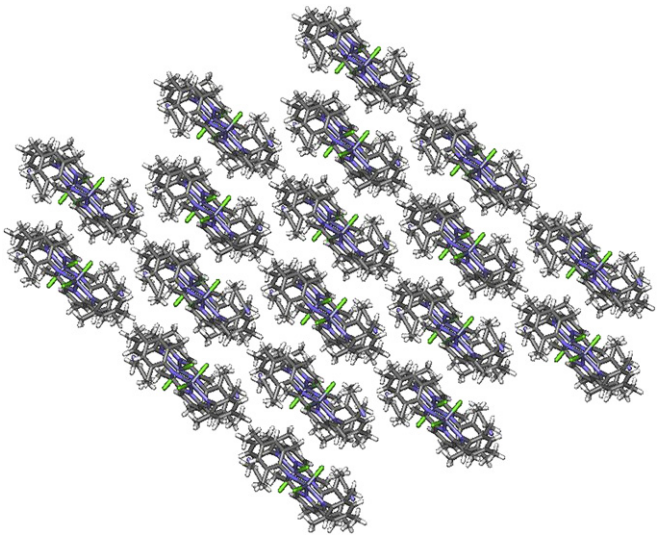

Fig. 8. The 3-D structure of complex Zn1 with π–π stacking interaction.

3.3. The relationship between crystal structures and electrochemical property

The X-ray structural analysis of the single-crystals reveals that compounds 1, 2 and 3 are isostructural. The complexes **Zn1**, **Cd1**, and **Hg1** possess the structures with an approximate C_s symmetry about a plane bisecting the central ptridine ring and containing the metal and two chlorides. As shown in Fig. 6 [30], the central atom is coordinated to five groups. The geometry about the central atom is a distorted trigonal bipyramid, which the equatorial plane is defined by the N(2)(pyridine), Cl(1), and Cl(2) atoms and the N(1) and N(3)(imino) atoms are in the axial position, in which M-C1(2)(M═Zn, Cd, and Hg) bond distances are significantly longer than M-N(2), moreover, M-N(3) bond distances are still longer than that of M-N(1). There are two independent molecules and one acetonitrile molecule in the asymmetric unit in the complexes. The dihedral angles in the **Zn1**, **Cd1**, and **Hg1** complexes between the phenyl rings and the plane formed by three coordinated nitrogen atoms are decreased with the proton number. The dihedral angles between the phenyl rings are oriented essentially orthogonal in **Zn1**, **Cd1**, and **Hg1**. The mean deviation of the metals in the complexes from the equatorial planes is 0.001, 0.013, and 0.022 Å, respectively, which means increase of distortion with the proton number. The axial M-N(imino) bonds subtending angles in **Zn1**, **Cd1**, and **Hg1** are equal 147.20(13)o, 138.27(11)o, and 135.3(2)o respectively, which means the decreasing. The metal atoms in **Zn1**, **Cd1**, and **Hg1** deviate by 0.100, 0.094, and 0.017 Å from the coordinated plane. They decrease with the proton numbers. The distances between metal and imino nitrogens are almost the same. Fig. 7 shows the packing diagram of **Zn1** along *c* axis. Hydrogen bonds are indicated by dashed lines. Fig. 8 shows the 3-D structure of complex **Zn1** with π–π stacking interaction. The electron-donating ability of the metal atom is in favor of stable single molecule structure between molecules. Therefore, the regular is that the decrease of the bond lengths and deviation distance are advantage in its electrochemical property, while the enlargement of the dihedral angles emerges superior cell performance.

4. Conclusions

In this paper, three transition metal-coordination complexes with pyridine-type ligands were designed and synthesized as the dye sensitizer for DSSC application. The results demonstrate the transition metal complexes with pyridine-type ligands lead to a significant increase in overall conversion efficiency of ZnO-based on dye-sensitized solar cell by co-sensitization with dye N719. Compared with the conventional electrode using dye N719, modification of ZnO electrode with the transition metal complexes and N719 not only extends the photoresponse of the electrode to the UV region of the solar spectrum, but also intensify the optical spectrum absorption. Co-adsorbing different dyes produce a competitive adsorption effect. The metal-coordination dyes provide a new design for development of DSSC technology.

Acknowledgments

This work was supported by the National Science Foundation of China (grant No. 21171044, 21071035 and 20971031), the China Postdoctoral Science Foundation funded project (No. 65204), and the Key Natural Science Foundation of the Heilongjiang Province, China (No. ZD201009).

References

[1] Minaev BF, Baryshnikov GV, Minaev VA. Electronic structure and spectral properties of the triarylamine–dithienosilole dyes for efficient organic solar cells. Dyes Pigm 2011;92:531–6.
[2] Blackburn OA, Coe BJ, Hahn V, Helliwell M, Raftery J, Ta YT, et al. *N*-Aryl stilbazolium dyes as sensitizers for solar cells. Dyes Pigm 2011;92:766–77.
[3] Baryshnikov GV, Minaev BF, Minaeva VA. Quantum-chemical study of effect of conjugation on structure and spectral properties of C105 sensitizing dye. Opt Spectrosc 2011;110(3):393–400.
[4] Fan S-Q, Kim C, Fang B, Liao K-X, Yang G-J, Li C-J, et al. Improved efficiency of over 10% in dye-sensitized solar cells with a ruthenium complex and an organic dye heterogeneously positioning on a single TiO_2 electrode. J Phys Chem C 2011;115:7747–54.
[5] Chen W, Zhang H, Hsing M, Yang S. A new photoanode architecture of dye sensitized solar cell based on ZnO nanotetrapods with no need for calcination. Electrochem Commun 2009;11:1057–60.
[6] Xu F, Dai M, Lu Y, Sun L. Hierarchical ZnO nanowire-nanosheet architectures for high power conversion efficiency in dye-sensitized solar cells. J Phys Chem C 2010;114:1776–82.
[7] Jiang CY, Sun XW, Lo GQ, Kwong DL. Improved dye-sensitized solar cells with a ZnO-nanoflower photoanode. Appl Phys Lett 2007;90:263501.
[8] Chen ZH, Tang YB, Liu CP, Leung YH, Yuan GD, Chen LM, et al. Vertically aligned ZnO nanorod arrays sentisized with gold nanoparticles for schottky barrier photovoltaic cells. J Phys Chem C 2009;113:13433–7.
[9] Peh CKN, Ke L, Ho GW. Modification of ZnO nanorods through Au nanoparticles surface coating for dye-sensitized solar cells applications. Mater Lett 2010;64:1372–5.
[10] Paksa P, Nilphai S, Gardchareon A, Choopun S. Copper oxide thin film and nanowire as a barrier in ZnO dye-sensitized solar cells. Thin Solid Film 2009; 517:4741–4.
[11] Plank NOV, Snaith HJ, Ducati C, Bendall JS, Schmidt-Mende L, Welland ME. A simple low temperature synthesis route for ZnO–MgO core–shell nanowires. Nanotechnol 2008;19:465603.
[12] Chen H, Pasquier AD, Saraf G, Zhong J, Lu Y. Dye-sensitized solar cells using ZnO nanotips and Ga-doped ZnO films. Semicond Sci Technol 2008;23: 045004.
[13] Kwak D-J, Kim J-H, Park B-W, Sung Y-M, Park M-W, Choo Y-B. Growth of ZnO: Al transparent conducting layer on polymer substrate for flexible film typed dye-sensitized solar cell. Curr Applied Phys 2010;10:S282–5.
[14] Tan B, Toman E, Li Y, Wu Y. Zinc stannate(Zn_2SnO_4) dye-sensitized solar cells. J Am Chem Soc 2007;129:4162–3.
[15] Zhang Q, Dandeneau CS, Park K, Liu D, Zhou X, Jeong Y-H, Cao G. Light scattering with oxide nanocrystallite aggregate for dye-sensitized solar cell application. J Nanophotonics 2010;4:041540.
[16] Zheng Y-Z, Tao X, Wang L-X, Xu H, Hou Q, Zhou W-L, et al. Novel ZnO-based film with double light-scattering layers as photoelectrodes for enhanced efficiency in dye-sensitized solar cells. Chem Mater 2010;22:928–34.
[17] Anderson NA, Ai X, Lian T. Electron injection dynamics from Ru polypyridyl complexes to ZnO nanocrystalline thin films. J Phys B 2003;107:14414–21.
[18] Bauer C, Boschloo G, Mukhtar E, Hafeldt A. Electron injection and recombination in $Ru(dcbpy)_2(NCS)_2$ sensitized nanostructured ZnO. J Phys Chem B 2001;105:5585–8.
[19] Horiuchi H, Katoh R, Hara K, Yanagida M, Murata S, Tachiya M. Electron injection efficiency from excited N3 into nanocrystalline ZnO films: effect of ($N3–Zn^{2+}$) aggregate formation. J Phys Chem B 2003;107:2570–4.

[20] Murai M, Furube A, Yanagida M, Hara K, Katoh R. Near-IR transient absorption spectra of N3 dye as a probe of aggregation on nanocrystalline semiconductor films. Chem Phys Lett 2006;423:417–21.
[21] Zhang R, Pan J, Briggs EP, Thtash M, Kerr LL. Studies on the adsorption of RuN3 dye on sheet-like nanostructured porous ZnO films. Sol Energy Mater Sol Cells 2008;92:425–31.
[22] Wong WY. Challenges in organometallic research – great opportunity for solar cells and OLEDs. J Organomet Chem 2009;494:2644–7.
[23] Wu W, Meng F, Li J, Teng X, Hua J. Co-sensitization with near-IR absorbing cyanine dye to improve photoelectric conversion of dye-sensitized solar cells. Synth Met 2009;159:1028–33.
[24] Chen Y, Zeng Z, Li C, Wang W, Zhang B. Highly efficient co-sensitization of nanocrystalline TiO_2 electrodes with plural organic dyes. New J Chem 2005; 29:773–6.
[25] Fang J, Mao H, Wu J, Zhang X, Lu Z. The photovoltaic study of co-sensitized microporous TiO_2 electrode with porphyrin and phthalocyanine molecules. Appl Surf Sci 1997;119:237–41.
[26] Ehret A, Stuhl L, Spitler MT. Spectral sensitization of TiO_2 nanocrystalline electrodes with aggregated cyanine dyes. J Phys Chem 2001;105:9960–5.
[27] Guo M, Diao P, Ren Y-J, Meng F, Tian H, Cai S-M. Photoelectrochemical studies of nanocrystalline TiO_2 co-sensitized by novel cyanine dyes. Sol Energy Mater Sol Cells 2005;88:23–5.
[28] Yum J-H, Jang S-R, Walter P, Geiger T, Nüesch F, Kim S. Efficient co-sensitization of nanocrystalline TiO_2 films by organic sensitizers. Chem Comm; 2007:4680–2.
[29] Fan R, Yang Y, Yin Y, Hasi W, Mu Y. Syntheses and structures of blue-luminescent mercury(II) complexes with 2,6-Bis(imino)pyridyl ligands. Inorg Chem 2009;48:6034–43.
[30] Fan RQ, Chen H, Wang P, Yin YB, Hasi W. Syntheses, structures, and luminescent properties of Zn(II) and Cd(II) complexes: 3-D supramolecules based on 2,6-bis(imino)pyridine ligands constructed by hydrogen bonding interactions. J Coord Chem 2010;63:1514–30.
[31] Zhong JY, Wang F. Modified synthetic methods of 2,6-diacetylpyridine. Acta Academiae Medicinae Jiangxi 1999;39:93–8.